ACS MATERIALS Au
AN OPEN ACCESS JOURNAL OF THE AMERICAN CHEMICAL SOCIETY

pubs.acs.org/materialsau

Article

Synthesis of Antimicrobial Gallium Nanoparticles Using the Hot Injection Method

Christina Limantoro, Theerthankar Das, Meng He, Dmitry Dirin, Jim Manos, Maksym V. Kovalenko, and Wojciech Chrzanowski*

Cite This: *ACS Mater. Au* 2023, 3, 310–320

Read Online

ACCESS | Metrics & More | Article Recommendations | Supporting Information

ABSTRACT: Antibiotic resistance continues to be an ongoing problem in global public health despite interventions to reduce antibiotic overuse. Furthermore, it threatens to undo the achievements and progress of modern medicine. To address these issues, the development of new alternative treatments is needed. Metallic nanoparticles have become an increasingly attractive alternative due to their unique physicochemical properties that allow for different applications and their various mechanisms of action. In this study, gallium nanoparticles (Ga NPs) were tested against several clinical strains of *Pseudomonas aeruginosa* (DFU53, 364077, and 365707) and multi-drug-resistant *Acinetobacter baumannii* (MRAB). The results showed that Ga NPs did not inhibit bacterial growth when tested against the bacterial strains using a broth microdilution assay, but they exhibited effects in biofilm production in *P. aeruginosa* DFU53. Furthermore, as captured by atomic force microscopy imaging, *P. aeruginosa* DFU53 and MRAB biofilms underwent morphological changes, appearing rough and irregular when they were treated with Ga NPs. Although Ga NPs did not affect planktonic bacterial growth, their effects on both biofilm formation and established biofilm demonstrate their potential role in the race to combat antibiotic resistance, especially in biofilm-related infections.

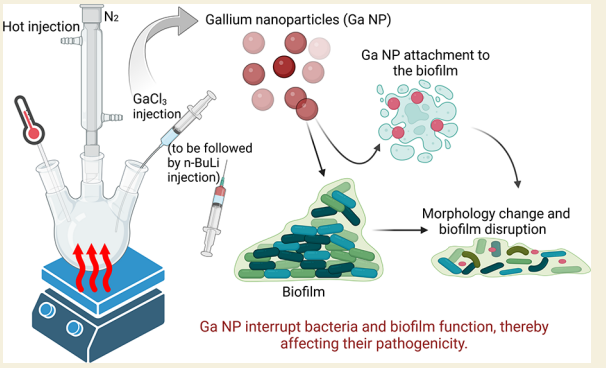

KEYWORDS: *gallium, nanoparticles, antimicrobial, biofilm, antibiotic-resistant bacteria*

Antibiotics, like a double-edged sword, have saved countless numbers of lives and given rise to the development of resistance that poses a global threat. Their discovery has revolutionized medicine; however, their use over the years has caused reduced efficacy and increased resistance development by many bacterial pathogens. While attempts such as stewardship programs have been made to optimize antibiotic use and minimize their impact on resistance development, antibiotic resistance remains among the top threats to public health that could undo achievements from modern medicine and put it to an end unless new alternatives are found.[1]

The use of metal-based nanoparticles (NPs) in the medical field has attracted much interest in recent years. By nanostructuring metals into nanomaterials, their physicochemical properties are altered, giving nanomaterials unique characteristics that are different from their original bulk materials.[2] Various metals have been made into NPs and investigated for their use as diagnostic tools and therapeutic agents. Among them, silver NPs are the most widely explored as antimicrobial agents. They have shown antimicrobial activity against different classes of bacteria and produce synergistic effects when used in combination with antibiotics.[3−5] Metal-based NPs are thought to be effective against bacteria that are resistant to traditional antibiotics because of their mechanism of action which differs from traditional antibiotics.[6] They often target multiple pathways, which does not entirely prevent the emergence of resistance, but it does make the development of it more difficult as the bacteria would have to build multiple defense mechanisms simultaneously.[6,7] As such, metal-based NPs offer a promising solution to the problem of antibiotic resistance.

Gallium (Ga) is a silvery-white metal that is widely used in the electronics industry and was initially developed for medical applications as diagnostics tools for tumor imaging.[8−10] Following recognition of their tendency to accumulate in growing tumors, Ga-based compounds were further developed into cancer therapeutic agents.[11−13] While the mechanisms of Ga uptake and anticancer activity are not entirely understood, they are likely related to Ga's similar chemical structure to iron that allows them to act as iron mimetics.[14] Ga can interfere

Received: December 11, 2022
Revised: March 13, 2023
Accepted: March 14, 2023
Published: March 28, 2023

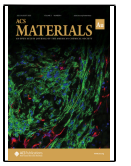

https://doi.org/10.1021/acsmaterialsau.2c00078
ACS Mater. Au 2023, 3, 310–320

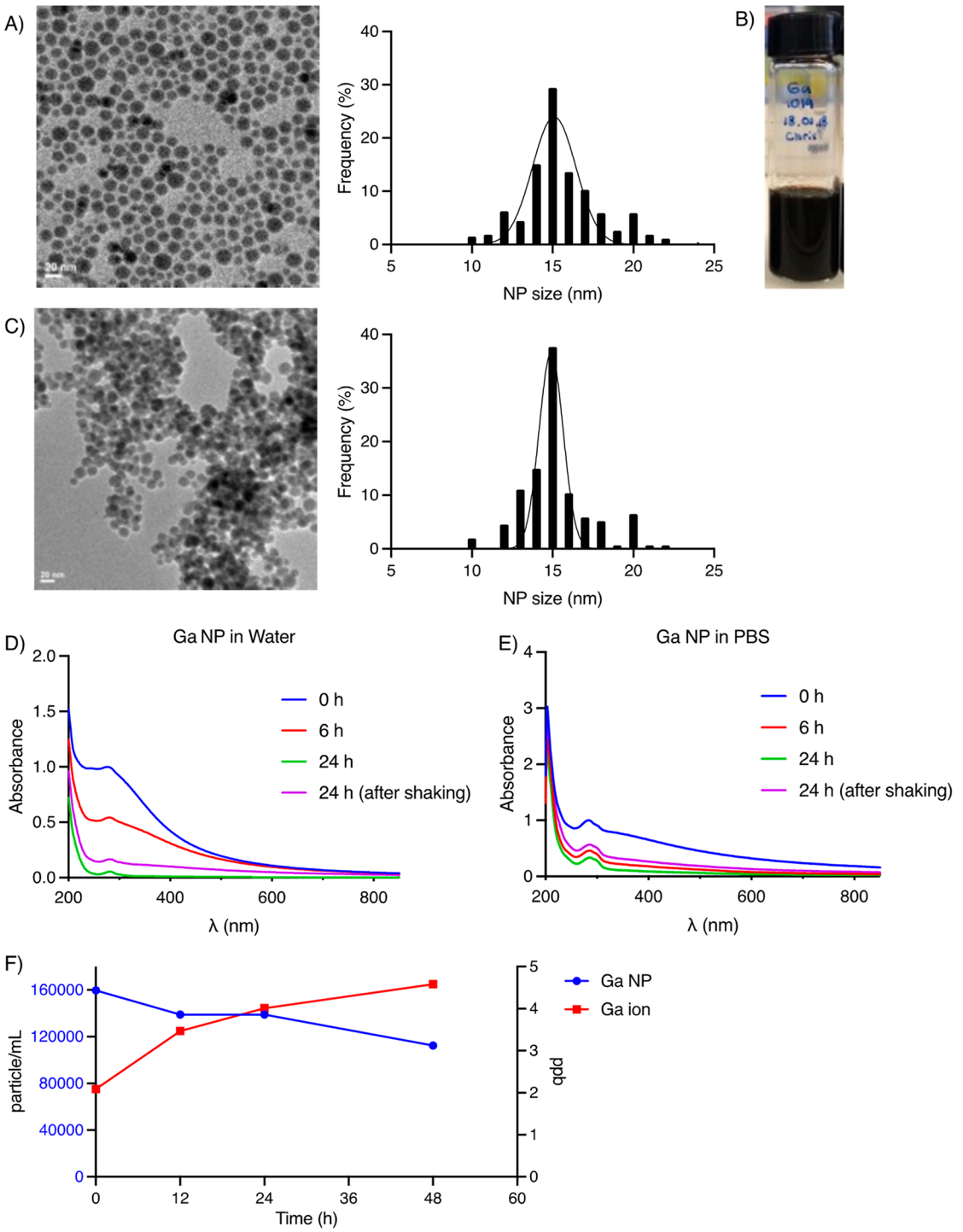

Figure 1. TEM images and size distribution graphs of nonfunctionalized (A) and functionalized (C) Ga NPs (scale bar = 20 nm). (B) Nonfunctionalized Ga NPs following overnight storage in chloroform. UV−vis absorption spectra of functionalized Ga NPs in water (D) and PBS (E). SP-ICP-MS measurement of functionalized Ga NPs and ion concentrations in PBS (F).

with iron-dependent processes because, unlike iron, Ga cannot be reduced in physiological conditions.[15,16] Since cancer cells are more proliferative than normal cells, they have an increased dependency on iron that makes them more susceptible to the effects of Ga.[17]

With the continuing problem associated with multi-drug resistance among pathogenic bacterial species, the discovery of new alternative antimicrobial agents has become more important now than ever. Ga-based compounds have received interest for their potential application in bacterial infections as they offer a unique solution to the problem by acting as an iron mimetic trojan horse. Like all living organisms, bacteria require iron for survival. They have developed various mechanisms for iron acquisitions within mammalian hosts where iron availability is limited as a part of the host's innate defense against invading pathogens. However, the bacterial iron uptake systems are practically unable to distinguish Ga from iron.[18−20] In a similar way that Ga exhibits its anticancer effects, it

https://doi.org/10.1021/acsmaterialsau.2c00078
ACS Mater. Au 2023, 3, 310−320

interrupts iron-dependent processes that are necessary for cellular function in the bacteria, ultimately resulting in cellular death. The development of resistance to Ga by reducing its uptake would therefore be challenging as it would also reduce iron uptake.[16,21] Ga-based compounds have exhibited efficacy against different bacterial pathogens including *Pseudomonas aeruginosa*, *Acinetobacter baumannii*, *Staphylococcus aureus*, *Rhodococcus equi*, *Escherichia coli*, and several mycobacterium species.[21−30] Additionally, they have shown ability to inhibit and disrupt *P. aeruginosa* biofilms.[22]

Despite the extensive potential medical applications of Ga, the progress to advance Ga-based compounds into clinical settings has largely been hindered by their low availability as they are extensively hydrolyzed to form insoluble hydroxide at physiological conditions.[31,32] Ga nitrate (Ganite), for example, is an FDA-approved drug for the treatment of cancer-related hypercalcemia. While this confirms the safety of Ga in clinical settings, a continuous 24 h a day intravenous infusion for 5−7 days is required for efficacy.[33,34] Formulating compounds into NPs has been shown to improve bioavailability and provide steady release of therapeutic agents.[35−37] As such, we hypothesized that formulating Ga into NPs will prolong and enhance their antimicrobial activity. The goal of this study was to synthesize Ga NPs using a hot injection method and functionalize them for dispersibility in aqueous media and then to demonstrate their antimicrobial and antibiofilm activities against clinical strains of *P. aeruginosa* and multi-drug-resistant *A. baumannii* (MRAB). To our knowledge, NPs made of only Ga synthesized via a hot injection have not previously been studied for their antimicrobial activity. The use of such NPs would indicate that the antimicrobial activity observed stems from Ga and highlights the novelty of this study.

RESULTS AND DISCUSSION

Ga NP Synthesis and Functionalization

Ga NPs were synthesized using gallium chloride as a metal precursor, *n*-butyllithium as a reducing agent, and oleylamine as a ligand, enabling colloidal stability of NPs in apolar solvents.[38] The resulting NPs were uniformly spherical, and their size distribution as determined from transmission electron microscopy (TEM) images ranged between 10 and 24 nm (Figure 1A). The median diameter of the NPs was 15 nm with 73% of the NPs being 13−17 nm. The NPs were stored in chloroform and remained in suspension after several weeks of storage at 4 °C, which suggests that they maintained colloidal stability (Figure 1B).

To achieve colloidal stability (dispersion) in aqueous solutions, Ga NPs were functionalized via ligand exchange following a previously reported method by Dragoman et al.[39] Several NP to ligand ratios were tested: 1:1, 1:2, 1:10, 2:1, and 4:1. While ligand exchange at 2:1 and 1:1 NP to ligand ratios produced water-dispersible NPs, dispersibility was further improved on Ga NPs functionalized at a 4:1 NP to ligand ratio. As shown through TEM imaging, the functionalized NPs ranged from 10 to 22 nm in size with a median of 15 nm, and 80% of them were 13−17 nm (Figure 1C). We also note that Ga NPs are expected to have an oxide shell because of Ga's eagerness toward oxidation. This shell is thin, approximately 1−2 monolayers, as it was not detected by X-ray diffraction, and its thinness is likely to further slowdown the release of Ga ions from the NPs.[38]

Functionalized Ga NPs were further analyzed using UV−vis spectrophotometry and single-particle inductively coupled plasma mass spectrometry (SP-ICP-MS) to quantify the concentration of Ga NPs and the amount of Ga ions in the solution. The samples were prepared in water and phosphate-buffered saline (PBS) to determine if the different solvents could affect colloidal stability, and their absorbance values at 300 nm were measured at several different time points. Both samples had the same pattern, where absorbance values decreased over time, which suggested a decrease in NP concentration (Figure 1D,E). The largest reduction in absorbance values occurred within the first 6 h of NP incubation in the solvent (54.8 and 43.5% for NPs in water and PBS, respectively). After 24 h of incubation, absorbance values were further reduced (96.8 and 69.4% for NPs in water and PBS, respectively), and the samples appeared clear with some brown precipitates visible at the bottom of the container. Upon shaking, absorbance values increased by 4.8 times for the sample in water and by 1.8 times for the sample in PBS. For the SP-ICP-MS experiment, functionalized Ga NPs were incubated in PBS for 0, 12, 24, and 48 h prior to analysis. The results showed a decrease in the number of NPs with longer incubation time, and the greatest concentration reduction (13%) was observed with Ga NPs that were incubated for 12 h (Figure 1F). The decrease in NP concentration was also accompanied by an increase in dissolved ion concentration from 2.09 to 4.58 ppb, with the highest concentration increase (66%) occurring in the 12 h incubated sample (Figure 1F). Although the overall changes in NP and dissolved ion concentrations were relatively small, the trends indicated that the rates of concentration change slowed down on samples that were incubated longer than 12 h prior to analysis. These results suggest that, after a burst release following 12 h incubation, ion release from the NPs occurred in a sustained manner.

Ga NPs were functionalized via ligand exchange to achieve colloidal stability in aqueous media. Hard oxygen-based ligands were considered according to the hard and soft acid base principle: Ga^{3+} is a hard acid, and hard acids favor interactions with hard bases such as oxygen.[40] Among various potential oxygen-based ligands, dopamine hydrochloride was selected due to its proven safety for clinical application as an FDA-approved drug.[41] Colloidal stability of Ga NPs was achieved via ligand exchange where a 4:1 NP to ligand ratio was most favorable, and the functionalization did not affect the size or shape of the NPs. To characterize the stability of the functionalized Ga NPs in aqueous solution, UV absorbance was measured at different time points. Absorbance value differences between functionalized Ga NPs in water and PBS suggest that the functionalized Ga NPs degrade in aqueous solution over time at different rates depending on the media in which they are dispersed.[42] Reduction in absorbance values is commonly attributed to reduced concentrations due to their linear relationship.[43] However, in the case of Ga NPs, NP sedimentation and oxidation are also contributing factors as the absorbance values increased following sample agitation but did not return to their initial values at 0 h incubation. Functionalized Ga NPs in PBS were used in the bacterial studies and thus further characterized through SP-ICP-MS. The results showed that the decrease in NP concentration was accompanied by an increase in the dissolved ion concentrations, and the rates of change decreased on samples that were incubated for 24 and 48 h before they were analyzed. The

https://doi.org/10.1021/acsmaterialsau.2c00078
ACS Mater. Au 2023, 3, 310−320

A)

Ga(III) (μg/mL)	48 h Incubated NP			
	DFU53	364077	365707	MRAB
400	+	+	+	+
200	+	+	+	+
100	+	+	+	+
50	+	+	+	+
10	+	+	+	+
5	+	+	+	+
Control	+	+	+	+

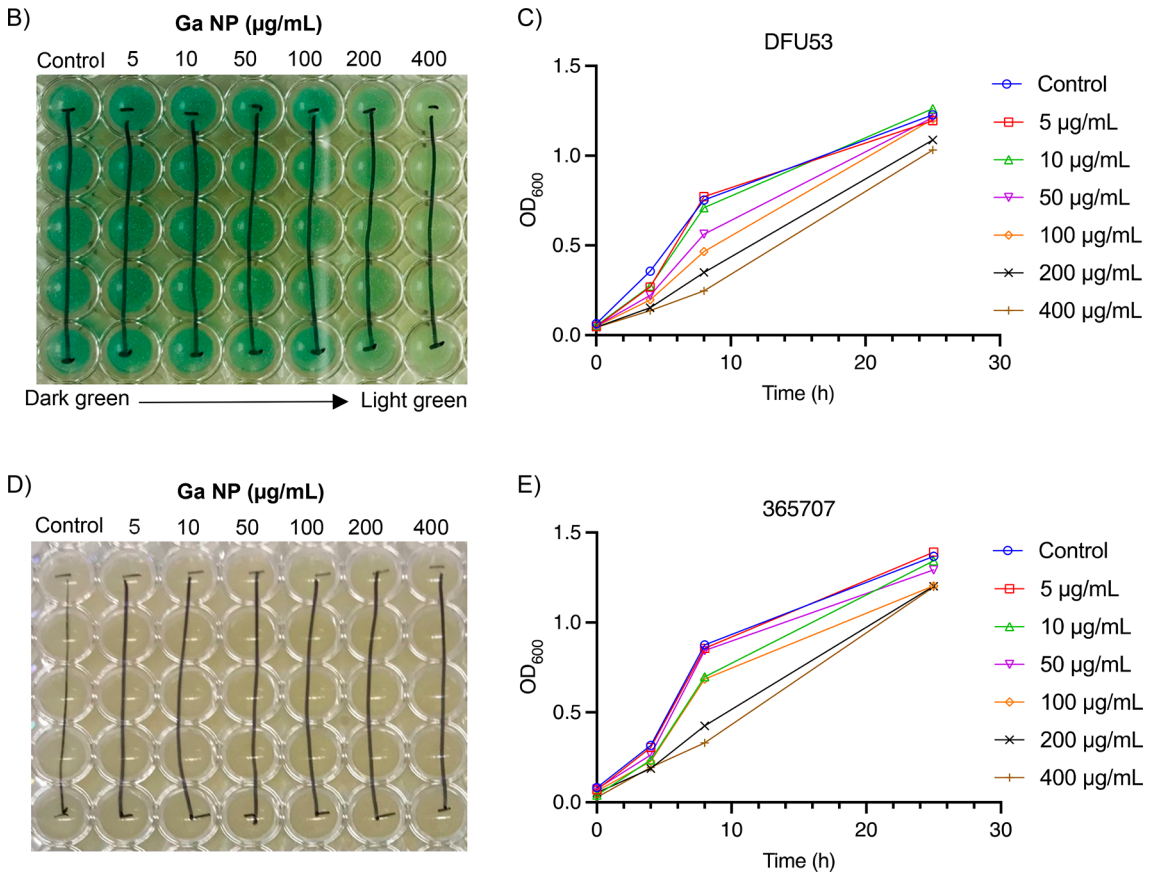

Figure 2. (A) Broth microdilution test of 48 h PBS-incubated Ga NPs against clinical strains of *P. aeruginosa* (DFU53, 364077, and 365707) and MRAB. Microdilution plate photographs of *P. aeruginosa* DFU53 (B) and 365707 (D) after 25 h treatment with 48 h PBS-incubated Ga NPs. *P. aeruginosa* DFU53 (C) and 365707 (E) growth as optical density measured at 600 nm at different time points.

ion release rate was fastest in 12 h incubated Ga NPs (5.5% increase per hour) followed by a sustained release rate on samples that were incubated for longer: 1.3 and 0.6% per hour for 24 and 48 h incubated samples (Figure 1F). The sustained ion release could be beneficial as it could reduce dosing frequency while maintaining concentration above the minimum inhibitory concentration. Therefore, to investigate the effect of NP decomposition and precipitation on their antimicrobial activity, functionalized Ga NPs were dispersed in PBS immediately (0 h incubation), 24 h, and 48 h before performing each antimicrobial experiment.

Antimicrobial Analysis of Ga NPs

The antimicrobial activity of functionalized Ga NPs was tested against several clinical strains of *P. aeruginosa* (DFU53, 364077, and 365707) and MRAB using the broth microdilution assay. *P. aeruginosa* strains were treated using functionalized Ga NPs dispersed in PBS immediately before use (0 h incubation) and after 24 and 48 h incubation to allow time for Ga NP decomposition.

Bacterial growth was observed in all tested *P. aeruginosa* strains across all concentrations; however, reduced growth as quantified by optical density (OD) measurement at 600 nm was observed in *P. aeruginosa* DFU53 and 365707 treated with Ga NPs that were incubated for 48 h in PBS before use (Figure

https://doi.org/10.1021/acsmaterialsau.2c00078
ACS Mater. Au 2023, 3, 310−320

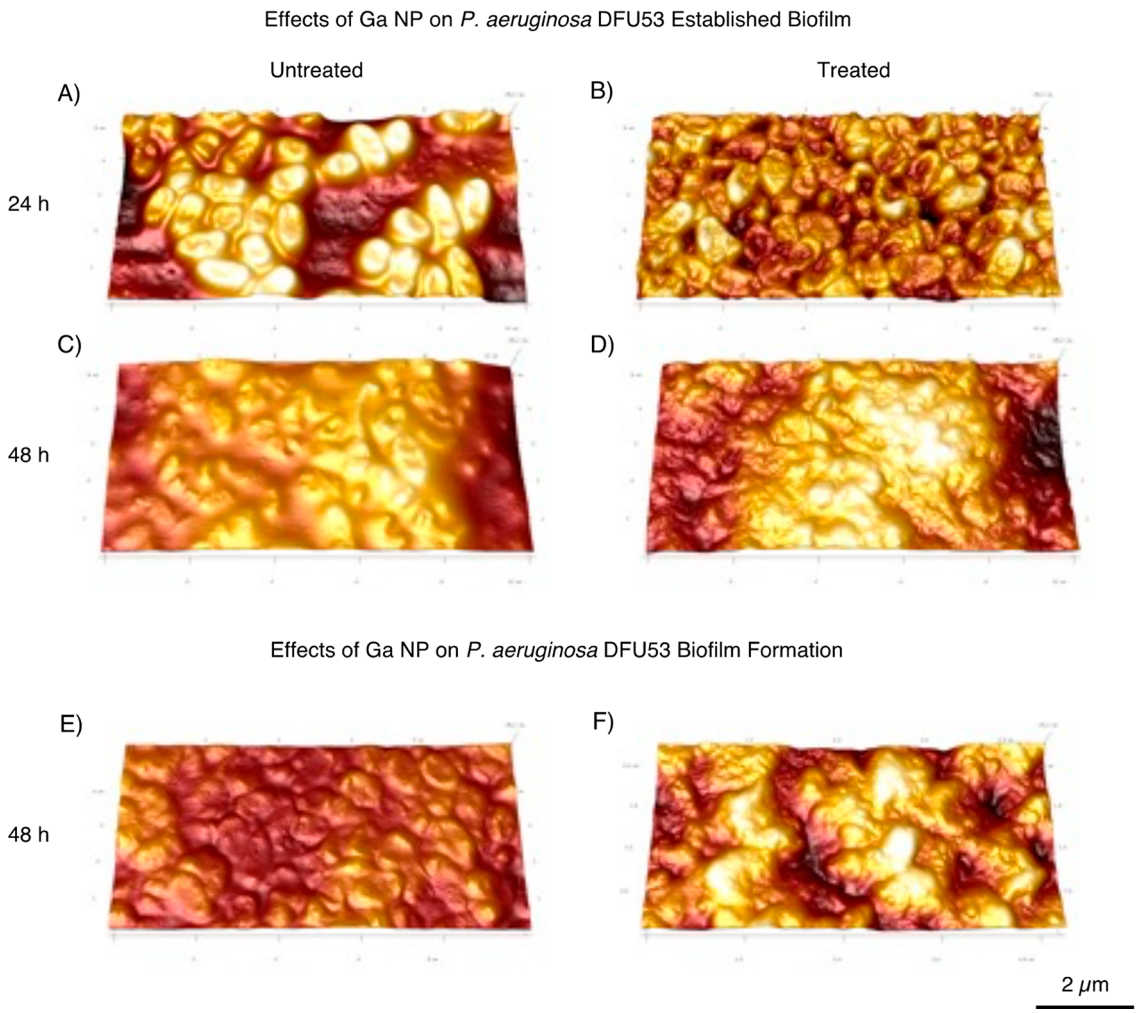

Figure 3. AFM images of *P. aeruginosa* DFU53 biofilm untreated (A,C) and treated (B,D) with 24 h PBS-incubated Ga NPs and those grown without (E) and with Ga NPs (F).

2A,C,E). The greatest growth reduction occurred at the third time point, after 8 h of treatment. *P. aeruginosa* DFU53 treated with ≥50 μg/mL Ga NPs were initially affected, but only those treated with 200 and 400 μg/mL showed reduced growth and a color change after 25 h of treatment upon visual inspection (Figure 2B). They adopted a lighter blue green color with increasing concentration of Ga NPs, which suggests that while Ga NPs did not prevent bacterial growth, they can still interfere with other bacterial processes. On *P. aeruginosa* 365707, growth was reduced at ≥100 μg/mL Ga NP treatment and remained reduced after 25 h of treatment, although to a lesser extent; however, color change on the cultures was absent (Figure 2D). Meanwhile, the effects of Ga NPs on MRAB were similar to those of *P. aeruginosa* 364077, where bacterial growth was observed and not reduced in all concentrations tested, and no color change on the culture was noted (Figure S1). The lack of these effects indicated that Ga NPs have different efficacies toward different types and strains of bacteria.

The broth microdilution assays performed using functionalized Ga NPs with 0 h incubation time showed bacterial growth in all tested bacterial strains and concentrations, despite the highest concentration tested (Ga NP 400 μg/mL = Ga(III) 297.57 μg/mL) being higher than the reported IC_{90} on *P. aeruginosa* and *A. baumannii* (Ga(III) 44.62 and 6.97 μg/mL, respectively).[44,45] Since the oxide shell on Ga NPs could slow down ion release from the NPs, the assays were also performed using functionalized Ga NPs incubated in PBS for 24 and 48 h. Although similar results where Ga NPs did not inhibit planktonic bacterial growth were noted, OD at t = 25 h was reduced on *P. aeruginosa* DFU53 and 365707 treated with 48 h PBS-incubated Ga NPs at ≥200 and ≥100 μg/mL, respectively. Reduction in OD indicates a decrease in bacterial density, which can interfere with quorum sensing.

Bacteria use quorum sensing to regulate gene expressions in response to changes in population density. The genes that quorum sensing control are involved in processes that benefit the whole population such as antibiotic production, virulence factor expressions, and biofilm formation to name a few.[46,47] In *P. aeruginosa*, these include genes that activate pyocanin biosynthesis, and studies have shown that quorum sensing inhibitors can prevent pyocyanin production and biofilm formation.[48−50] The blue-green color on *P. aeruginosa* is indicative of pyocyanin biosynthesis, a virulence factor involved in pathogenicity and biofilm formation.[51] It intercalates with the extracellular DNA in *P. aeruginosa* biofilm matrix to stabilize the biofilm and is essential for *P. aeruginosa* viability under hypoxic conditions.[52−54] *P. aeruginosa* strains that are pyocyanin deficient have been shown to produce weaker biofilms.[52,53] Among the 3 *P. aeruginosa* strains that

https://doi.org/10.1021/acsmaterialsau.2c00078
ACS Mater. Au 2023, 3, 310−320

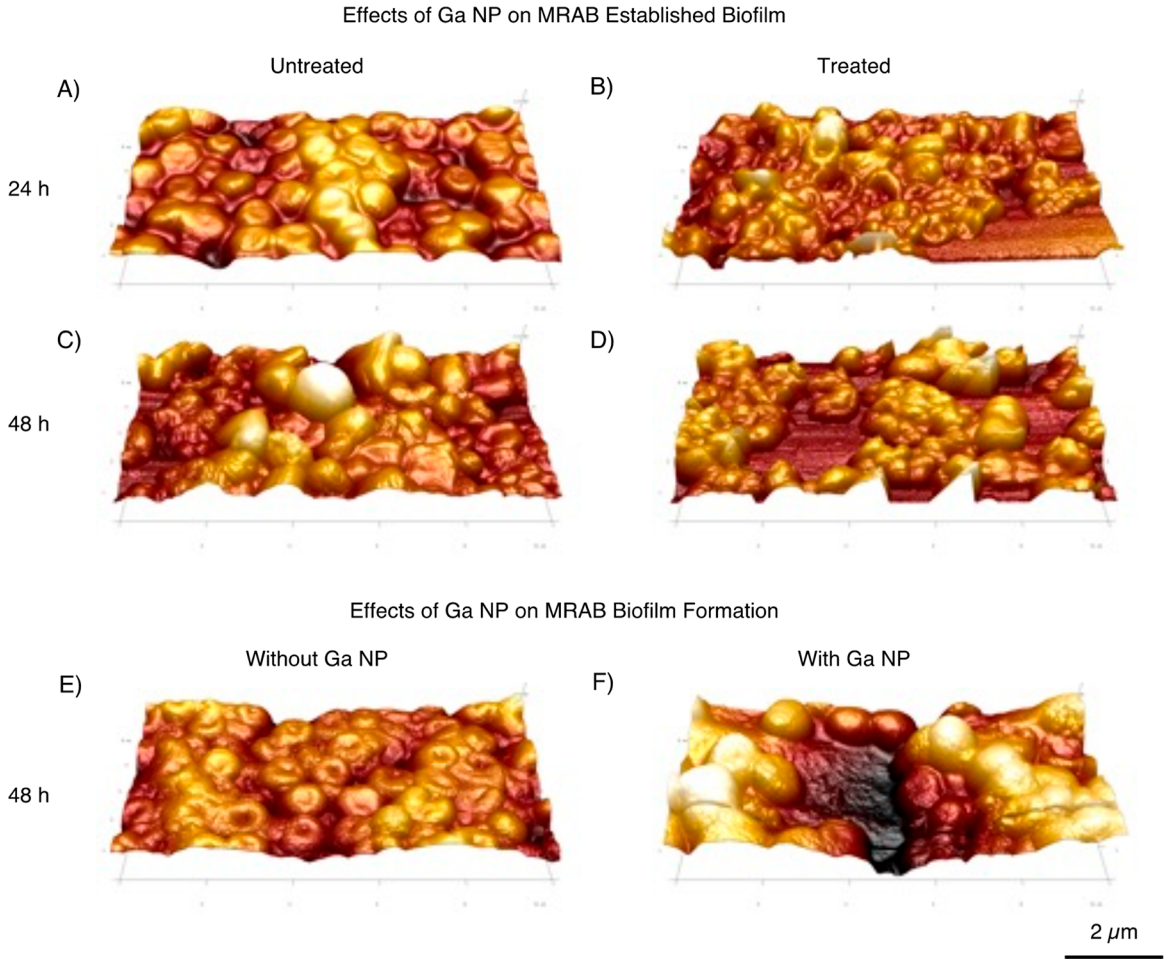

Figure 4. AFM images of MRAB biofilm untreated (A,C) and treated (B,D) with 24 h PBS-incubated Ga NPs and those grown without (E) and with Ga NP (F).

were tested, only *P. aeruginosa* DFU53 produced pyocyanin, as indicated by their blue-green color. At Ga NP concentrations where bacterial growth was reduced (200 and 400 μg/mL), a lighter blue-green color was also observed on the culture. These results suggest that Ga NPs can reduce bacterial growth in specific *P. aeruginosa* strains, and in pyocyanin producing strains, this could affect pyocyanin biosynthesis through quorum sensing which can impair biofilm formation. Furthermore, as the effects of Ga NPs were only observed on the cultures treated using 48 h PBS-incubated Ga NPs, it suggests that the effects of Ga NPs are linked to their decomposition and ion release. The loss of activity on planktonic bacteria as a result of nanoformulation has also been reported in a study where antimicrobial soluble copper was found to have negligible antimicrobial effects when formulated into nanoparticles.[55] Given Ga's mechanism of action, the use of iron-rich media in the study could also explain the lack of planktonic growth inhibition by Ga NPs as it provides a competitive binding environment.[16] This is further supported by several studies which have shown increased antimicrobial activity by Ga in a low iron environment and reduced activity in a high iron environment.[21,23,26,44,45]

Antibiofilm Analysis of Ga NPs

P. aeruginosa DFU53 and MRAB were used as model bacteria to investigate the effects of functionalized Ga NPs on established biofilm and biofilm formation. Here, 400 μg/mL functionalized Ga NPs dispersed and incubated in PBS for 24 h was used as the treatment, and AFM imaging was used for morphological analysis.

On established *P. aeruginosa* DFU53 biofilm, 24 and 48 h treatment with Ga NPs resulted in changes on the bacteria and biofilm morphologies. After 24 h treatment, the bacteria appeared "shriveled" and had a rough surface, losing their rod-shaped morphology (Figure 3A,B). Prolonged treatment (48 h) altered the biofilm morphology from smooth and even to irregular and uneven (Figure 3C,D). Additionally, untreated biofilm appeared to have a thicker matrix deposition in comparison to that of the Ga NP treated biofilm.

Biofilm morphological changes were also observed in *P. aeruginosa* DFU53 grown with Ga NPs for 48 h. Whereas untreated bacteria appeared to be covered by a smooth layer of biofilm, treated bacteria grew irregular biofilm and individual cell outlines could not be defined (Figure 3E,F).

Similar to *P. aeruginosa* DFU53, 24 h treatment on established biofilm of MRAB resulted in bacteria morphological changes. Bacteria in untreated biofilm had a typical short rod morphology, but upon 24 h treatment with Ga NPs, they lost their morphological uniformity, adopting a shriveled and irregular appearance (Figure 4A,B). Extending treatment time to 48 h did not result in further changes or striking differences between untreated and treated biofilms (Figure 4C,D). However, growing the MRAB biofilm in the presence

https://doi.org/10.1021/acsmaterialsau.2c00078
ACS Mater. Au 2023, 3, 310−320

of Ga NPs for 48 h resulted in morphological changes where multiple bacterial cells appeared to have aggregated and formed cellular clusters (Figure 4E,F). These results indicate that while Ga NPs did not inhibit MRAB growth, they have the capacity to damage the bacterial cellular morphology and biofilm formation.

To investigate the effects of Ga NPs on biofilm, *P. aeruginosa* DFU53 was selected among other *P. aeruginosa* strains due to their tendency to form biofilm, as indicated by their blue-green color. On the other hand, MRAB was selected to determine whether the biofilm effects of Ga NPs were limited to a specific bacteria type. In both *P. aeruginosa* DFU53 and MRAB biofilms, 24 h treatment with Ga NPs resulted in morphological loss of individual cells. Following an additional 24 h incubation, biofilm formation occurred in *P. aeruginosa* DFU53, and the effects of Ga NPs became evident on the biofilm morphology. Whereas the untreated biofilm appeared smooth, the treated biofilm appeared rough and irregular. However, unlike *P. aeruginosa* DFU45, biofilm formation was not observed in 48 h treated and untreated MRAB. Factors such as growth conditions, culture concentrations, ions, and nutrient availability can influence cell-to-cell communication and gene expression in bacteria that determine biofilm formation.[56−58] The lack of biofilm formation by MRAB suggests that the same conditions that supported biofilm formation in *P. aeruginosa* DFU45 was insufficient for MRAB biofilm formation. Cellular morphological changes observed in 48 h untreated MRAB in comparison to the 24 h untreated culture could be attributed to bacterial overgrowth that caused them to grow on top of each other.[59,60]

In addition to established biofilms, the effects of functionalized Ga NPs were investigated on biofilm formation by growing the bacterial culture with Ga NPs for 48 h, where similar results were observed. Biofilm formed by treated *P. aeruginosa* DFU53 appeared rough, irregular, and significantly different in comparison to the untreated culture. The outline of individual bacterial cell that was visible beneath the biofilm in the untreated culture also can no longer be distinguished. These results depicting damage on biofilm formation further support findings on the previous section that the lighter blue-green color on *P. aeruginosa* DFU53 treated with 400 μg/mL Ga NPs can be related to reduced pyocyanin biosynthesis, which is an important factor in biofilm formation (Figures 2B and 3E,F). While biofilm formation was not evident in MRAB, their cellular morphology was altered when the culture was grown in the presence of Ga NPs. Overall, the results in this study have shown that while Ga NPs did not inhibit planktonic bacterial growth, they could affect bacterial morphology and biofilm morphology in both established biofilms and biofilm formation. The results were beyond our expectation as bacteria in biofilms are known to be more resistant to antimicrobial agents.[61] Much higher concentrations are often required to generate effects on biofilm. However, here, at the same concentration where planktonic growth was observed, bacterial and biofilm morphologies as well as biofilm formation were affected, which suggests that direct interactions between Ga NPs and bacterial cells is likely to contribute to their efficacy.

Although the mechanism is not well understood, several compounds have also been found to have antibiofilm effects without any effects on bacteria in their planktonic form.[62−64] In a study by Harrison et al., metalloid tellurium reduction was found to be different between bacteria in planktonic and biofilm forms, and it resulted in the latter being susceptible to the compound.[65] Quorum sensing inhibitors have been known to reduce the virulence of pathogenic bacteria without killing them.[48,49,66] The ability to reduce virulence such as by impairing biofilm formation without killing the bacteria could be advantageous as it could prevent the eradication of otherwise normal and healthy microflora. More importantly, it could also put less pressure on resistance development. The effects of Ga NPs on biofilms demonstrate their potential applications in biofilm-related infections which has been on the rise with the increased use of medical device implants.[67] Similar to the use of Ga bioactive glasses for substrate coating, Ga NPs could also potentially be used for coating medical device implants.[68,69] However, the synthesis of Ga NPs via hot injection would be more favorable as synthesis of bioactive glasses often requires extremely high temperatures. Melt-derived synthesis of bioactive glasses requires precursor melting at 1000−1400 °C, while sol−gel derived synthesis of bioactive glasses requires calcination at approximately 700 °C.[70] On the other hand, Ga NPs synthesized using hot injection can be produced at 250 °C, making it a more feasible synthesis method.

CONCLUSION

Ga was formulated into NPs to investigate whether it could enhance its antimicrobial activity. The results showed that Ga NPs can affect *P. aeruginosa* and MRAB bacterial morphologies without inhibiting their planktonic growth. Furthermore, they could also alter the biofilm formation of selective bacteria. Since morphology relates to function, these results suggest that Ga NPs can interrupt bacteria and biofilm function, thereby affecting their pathogenicity. They can be expected to increase the efficacy of traditional antibiotics in biofilm-related infections when used in conjunction. More studies are required to further understand the mechanisms of Ga NPs; however, this study has highlighted the potential use of Ga to specifically target biofilms through the use to nanotechnology.

MATERIALS AND METHODS

Materials

Gallium chloride (99,999% anhydrous, ABCR), octadecene (ODE, 90%, Sigma-Aldrich), dioctylamine (DOA, 98%, Sigma-Aldrich), toluene (99.9%, Sigma-Aldrich), *n*-butyllithium in heptane (*n*-BuLi, 2.7 M, Sigma-Aldrich), oleylamine (OLA, tech., TCI), oleic acid (OA, 90%, Sigma-Aldrich), ethanol (≥99.9%, Scharlau), chloroform (≥99.8%, Sigma-Aldrich), dopamine hydrochloride (DA, Sigma-Aldrich), methanol (MeOH, Fisher Scientific), ethyl acetate (Fisher Scientific), phosphate-buffered saline (Sigma-Aldrich), Luria−Bertani broth (LB, Invitrogen, Life Technologies), and Tryptone soy broth (TSB, Oxoid, Thermo Fisher Scientific) were used.

Ga NP Synthesis and Functionalization

Ga NP synthesis was performed using a Schlenk line under a nitrogen atmosphere according to the protocol of He et al.[38] Briefly, 9 mL ODE and 1.13 mL DOA were added into a 50 mL three-neck flask and dried under vacuum at 110 °C for 1 h while stirring. Under N_2, the temperature was increased to 250 °C, followed by injections of $GaCl_3$ (0.066 g in 1 mL toluene) and *n*-BuLi (1.33 mL). Once the solution color changes from yellow to brown, which indicates NP formation, the reaction was quickly cooled to room temperature by air cooling, chloroform injection (6 mL at 190 °C and 4 mL at room temperature), OLA/OA injection (0.3 mL each at 50 °C), and an ice water bath. Ga NPs were then precipitated by adding 20 mL of ethanol and centrifugation at 9000 rpm for 5 min. The final Ga NPs were dispersed in chloroform.

https://doi.org/10.1021/acsmaterialsau.2c00078
ACS Mater. Au 2023, 3, 310−320

For Ga NP functionalization via ligand exchange, Ga NPs in chloroform were mixed with dopamine hydrochloride in methanol at different ratios (1:1, 1:2, 1:10, 2:1, and 4:1) in a 50 °C water bath overnight. They were then centrifuged at 13400 rpm for 1 min and redispersed in methanol. Ethyl acetate (3× the volume of methanol) was added to remove excess of unbound ligands, followed by another round of centrifugation. Finally, the functionalized Ga NPs were dispersed in water or PBS.

Ga NP Characterization

TEM (Philips CM30) was used to characterize nonfunctionalized and functionalized Ga NPs. The samples were prepared by placing a 10 μL droplet of the Ga NPs in solution on a 400-mesh carbon-coated copper grid and then dried prior to imaging. In addition to TEM, functionalized Ga NPs were also characterized using a Cary 5000 UV−vis spectrophotometer. The samples were prepared in water and PBS, and UV−vis absorption spectra were measured at different time points.

To measure dissolved ion concentrations and the number of nanoparticles in the solution, we used single-particle inductively coupled plasma mass spectroscopy (NexION 2000, PerkinElmer). The samples were prepared by incubating functionalized Ga NPs in PBS for 0, 12, 24, and 48 h. They were further diluted immediately prior to the elemental analysis with SP-ICP-MS. The instrument was calibrated using a multielement standard for the dissolved ion calibration and with 30, 50, and 100 nm gold NP standards (PerkinElmer) for the particle calibrations. The sample measurements were conducted using the single-particle mode.

Bacterial Strains and Culture Conditions

Clinical strains of *P. aeruginosa* were isolated from diabetic foot ulcer (DFU53, Liverpool Hospital, Australia), scalp wound (364077), and ankle wound (365707) of patients at Royal Prince Alfred Hospital in Sydney, Australia. The strains were deidentified before they were gifted to our research group, and they were cultured in LB broth media at 37 °C for 16 h with shaking (150 rpm) for experimental purposes. Multi-drug-resistant *A. baumanii* (MRAB) was isolated from a patient's wound at Concord Hospital (Sydney, Australia) and similarly deidentified before given to us. The isolate was maintained in TSB at 37 °C for 16 h with shaking (150 rpm).

Antimicrobial Analysis of Ga NPs

The broth microdilution method was used to investigate the activity of functionalized Ga NPs on planktonic growth of bacteria. Overnight grown culture was diluted appropriately to OD_{600} = 0.1 ± 0.02 and added into a 96-well microplate (200 μL per well). 50 μL of functionalized Ga NPs in PBS was then added to each well, and the microplate was incubated at 37 °C for 24 h with shaking. Bacterial growth was determined through visual inspection of the microplate for turbidity and confirmed by checking their optical density at 600 nm using a microplate spectrophotometer (Tecan Infinite M1000 Pro).

Antibiofilm Analysis of Ga NPs

Biofilms were grown on 13 mm round Thermanox coverslips in a 24-well microplate using 30 μL of overnight grown culture diluted with 370 μL of appropriate broth. They were grown in a shaking incubator at 37 °C for 48 h to allow biofilm formation. PBS wash was performed to remove loosely bound bacteria, and 80 μL of functionalized Ga NPs in PBS diluted with 320 μL of appropriate broth was then added. The microplate was returned into the shaking incubator for a further 24 or 48 h, after which the Thermanox coverslips were collected and analyzed using atomic force microscopy (AFM).

In a similar way, functionalized Ga NPs were investigated for their ability to prevent biofilm formation. Each culture was grown with or without the addition of functionalized Ga NPs on Thermanox coverslips in a 24-well microplate for 48 h. The Thermanox coverslips were then collected and analyzed using AFM.

Bacteria and Biofilm Analysis Using Atomic Force Microscopy

Collected Thermanox coverslips on which biofilms were grown were fixed on AFM metal stubs using superglue. They were air-dried then imaged using the Soft Tapping mode on a Multimode VIII AFM (Bruker). A minimum of three areas at different sizes (15 × 7.5 μm, 10 × 5 μm, and 5 × 2.5 μm) on each sample was captured at a 0.5 Hz scan rate using silicone tips (Olympus AC160TS; frequency 300 (200−400) kHz; spring constant k = 42 (12−103) N/m).

■ ASSOCIATED CONTENT

Supporting Information

The Supporting Information is available free of charge at https://pubs.acs.org/doi/10.1021/acsmaterialsau.2c00078.

Microdilution plate photographs and optical density measurements of *P. aeruginosa* 364077 and MRAB treated with Ga NPs (PDF)

■ AUTHOR INFORMATION

Corresponding Author

Wojciech Chrzanowski − *Sydney Pharmacy School, Faculty of Medicine and Health, The University of Sydney, Sydney, NSW 2006, Australia; Sydney Nano Institute, The University of Sydney, Sydney, NSW 2006, Australia;* orcid.org/0000-0001-8050-8821; Email: wojciech.chrzanowski@sydney.edu.au

Authors

Christina Limantoro − *Sydney Pharmacy School, Faculty of Medicine and Health, The University of Sydney, Sydney, NSW 2006, Australia; Sydney Nano Institute, The University of Sydney, Sydney, NSW 2006, Australia*

Theerthankar Das − *Department of Infectious Diseases and Immunology, School of Medical Sciences, The University of Sydney, Camperdown, NSW 2006, Australia;* orcid.org/0000-0003-0581-6060

Meng He − *Department of Chemistry and Applied Biosciences, ETH Zürich—Swiss Federal Institute of Technology Zürich, CH-8093 Zürich, Switzerland; Empa-Swiss Federal Laboratories for Materials Science and Technology, CH-8600 Dübendorf, Switzerland*

Dmitry Dirin − *Department of Chemistry and Applied Biosciences, ETH Zürich—Swiss Federal Institute of Technology Zürich, CH-8093 Zürich, Switzerland; Empa-Swiss Federal Laboratories for Materials Science and Technology, CH-8600 Dübendorf, Switzerland*

Jim Manos − *Department of Infectious Diseases and Immunology, School of Medical Sciences, The University of Sydney, Camperdown, NSW 2006, Australia*

Maksym V. Kovalenko − *Department of Chemistry and Applied Biosciences, ETH Zürich—Swiss Federal Institute of Technology Zürich, CH-8093 Zürich, Switzerland; Empa-Swiss Federal Laboratories for Materials Science and Technology, CH-8600 Dübendorf, Switzerland;* orcid.org/0000-0002-6396-8938

Complete contact information is available at: https://pubs.acs.org/10.1021/acsmaterialsau.2c00078

Author Contributions

CRediT: **Christina Limantoro** investigation (lead), writing-original draft (lead), writing-review & editing (lead); **Theerthankar Das** formal analysis (supporting), investigation

(supporting), methodology (supporting), supervision (supporting), writing-original draft (supporting), writing-review & editing (supporting); **Meng He** investigation (supporting), methodology (supporting); **Dmitry Dirin** investigation (supporting), methodology (supporting), writing-review & editing (supporting); **Jim Manos** writing-review & editing (supporting); **Maksym V. Kovalenko** investigation (supporting), resources (supporting), supervision (supporting), writing-original draft (supporting), writing-review & editing (supporting); **Wojciech Chrzanowski** conceptualization (equal), funding acquisition (equal), investigation (supporting), methodology (equal), project administration (lead), writing-original draft (supporting), writing-review & editing (supporting).

Notes

The authors declare no competing financial interest.

■ ACKNOWLEDGMENTS

We sincerely thank Dr. Matthew Malone of the Department of High-Risk Foot Service at Liverpool Hospital in Sydney and Southwestern Sydney Limb Preservation and Wound Research Academic Unit for gifting the *P. aeruginosa* DFU isolate and the Microbiology Department of Royal Prince Alfred Hospital for the *P. aeruginosa* isolates. We also extend our thanks to Dr. Tom Gottlieb and Dr. John Merlino of the Microbiology Department at Concord Hospital, NSW, for providing us with the multi-drug-resistant *A. baumannii* (MRAB) isolate for research purposes.

■ REFERENCES

(1) Sugden, R.; Kelly, R.; Davies, S. Combatting antimicrobial resistance globally. *Nature Microbiology.* **2016**, *1*, 16187.
(2) Khan, I.; Saeed, K.; Khan, I. Nanoparticles: Properties, applications and toxicities. *Arabian journal of chemistry.* **2019**, *12* (7), 908−31.
(3) Ipe, D. S.; Kumar, P. T. S.; Love, R. M.; Hamlet, S. M. Silver Nanoparticles at Biocompatible Dosage Synergistically Increases Bacterial Susceptibility to Antibiotics. *Front Microbiol.* **2020**, *11*, 1074.
(4) Ramalingam, B.; Parandhaman, T.; Das, S. K. Antibacterial Effects of Biosynthesized Silver Nanoparticles on Surface Ultrastructure and Nanomechanical Properties of Gram-Negative Bacteria viz. Escherichia coli and Pseudomonas aeruginosa. *Acs Applied Materials & Interfaces.* **2016**, *8* (7), 4963−76.
(5) Kim, J. S.; Kuk, E.; Yu, K. N.; Kim, J. H.; Park, S. J.; Lee, H. J.; et al. Antimicrobial effects of silver nanoparticles. *Nanomedicine-Nanotechnology Biology and Medicine.* **2007**, *3* (1), 95−101.
(6) Slavin, Y. N.; Asnis, J.; Häfeli, U. O.; Bach, H. Metal nanoparticles: understanding the mechanisms behind antibacterial activity. *Journal of nanobiotechnology.* **2017**, *15* (1), 65.
(7) Wang, L. L.; Hu, C.; Shao, L. Q. The antimicrobial activity of nanoparticles: present situation and prospects for the future. *Int. J. Nanomed.* **2017**, *12*, 1227−49.
(8) Moskalyk, R. R. Gallium: the backbone of the electronics industry. *Minerals Engineering.* **2003**, *16* (10), 921−9.
(9) Edwards, C. L.; Hayes, R. L. Tumor Scanning with 67Ga Citrate. *J. Nucl. Med.* **1969**, *10* (2), 103−105.
(10) Hoffer, P. Status of gallium-67 in tumor detection. *J Nucl. Med.* **1980**, *21* (4), 394−8.
(11) Chitambar, C. R. The therapeutic potential of iron-targeting gallium compounds in human disease: From basic research to clinical application. *Pharmacol. Res.* **2017**, *115*, 56−64.
(12) Einhorn, L. Gallium nitrate in the treatment of bladder cancer. *Seminars in Oncology.* **2003**, *30* (2Suppl 5), 34−41.
(13) Straus, D. J. Gallium nitrate in the treatment of lymphoma. *Seminars in oncology.* **2003**, *30* (2Suppl 5), 25.
(14) Jakupec, M. A.; Keppler, B. K. Gallium in cancer treatment. *Curr. Top Med. Chem.* **2004**, *4* (15), 1575−83.
(15) Bernstein, L. R. Mechanisms of therapeutic activity for gallium. *Pharmacol Rev.* **1998**, *50* (4), 665−82.
(16) Chitambar, C. R. Gallium and its competing roles with iron in biological systems. *Biochim Biophys Acta-Mol. Cell Res.* **2016**, *1863* (8), 2044−53.
(17) Jung, M.; Mertens, C.; Tomat, E.; Brüne, B. Iron as a Central Player and Promising Target in Cancer Progression. *Int. J. Mol. Sci.* **2019**, *20* (2), 273.
(18) Caza, M.; Kronstad, J. W. Shared and distinct mechanisms of iron acquisition by bacterial and fungal pathogens of humans. *Frontiers in Cellular and Infection Microbiology.* **2013**, *3*, 80.
(19) Emery, T. Exchange of Iron by Gallium in Siderophores. *Biochemistry.* **1986**, *25* (16), 4629−33.
(20) Frangipani, E.; Bonchi, C.; Minandri, F.; Imperi, F.; Visca, P. Pyochelin Potentiates the Inhibitory Activity of Gallium on Pseudomonas aeruginosa. *Antimicrobial Agents and Chemotherapy.* **2014**, *58* (9), 5572−5.
(21) Goss, C. H.; Kaneko, Y.; Khuu, L.; Anderson, G. D.; Ravishankar, S.; Aitken, M. L. Gallium disrupts bacterial iron metabolism and has therapeutic effects in mice and humans with lung infections. *Science translational medicine.* **2018**, *10* (460), eaat7520.
(22) Kaneko, Y.; Thoendel, M.; Olakanmi, O.; Britigan, B. E.; Singh, P. K. The transition metal gallium disrupts Pseudomonas aeruginosa iron metabolism and has antimicrobial and antibiofilm activity. *J. Clin Invest.* **2007**, *117* (4), 877−88.
(23) Antunes, L. C. S.; Imperi, F.; Minandri, F.; Visca, P. In Vitro and In Vivo Antimicrobial Activities of Gallium Nitrate against Multidrug-Resistant Acinetobacter baumannii. *Antimicrobial Agents and Chemotherapy.* **2012**, *56* (11), 5961−70.
(24) Yamaguchi, S.; Nath, S.; Sugawara, Y.; Divakarla, K.; Das, T.; Manos, J.; et al. Two-in-One Biointerfaces-Antimicrobial and Bioactive Nanoporous Gallium Titanate Layers for Titanium Implants. *Nanomaterials.* **2017**, *7* (8), 229.
(25) Arnold, C. E.; Bordin, A.; Lawhon, S. D.; Libal, M. C.; Bernstein, L. R.; Cohen, N. D. Antimicrobial activity of gallium maltolate against Staphylococcus aureus and methicillin-resistant S. aureus and Staphylococcus pseudintermedius: An in vitro study. *Vet. Microbiol.* **2012**, *155* (2−4), 389−94.
(26) Baldoni, D.; Steinhuber, A.; Zimmerli, W.; Trampuz, A. In Vitro Activity of Gallium Maltolate against Staphylococci in Logarithmic, Stationary, and Biofilm Growth Phases: Comparison of Conventional and Calorimetric Susceptibility Testing Methods. *Antimicrobial Agents and Chemotherapy.* **2010**, *54* (1), 157−63.
(27) Harrington, J. R.; Martens, R. J.; Cohen, N. D.; Bernstein, L. R. Antimicrobial activity of gallium against virulent Rhodococcus equiin vitro and in vivo. *Journal of veterinary pharmacology and therapeutics.* **2006**, *29* (2), 121−7.
(28) Xu, Z.; Zhao, X.; Chen, X.; Chen, Z.; Xia, Z. Antimicrobial effect of gallium nitrate against bacteria encountered in burn wound infections. *RSC Adv.* **2017**, *7* (82), 52266−73.
(29) Olakanmi, O.; Kesavalu, B.; Pasula, R.; Abdalla, M. Y.; Schlesinger, L. S.; Britigan, B. E. Gallium Nitrate Is Efficacious in Murine Models of Tuberculosis and Inhibits Key Bacterial Fe-Dependent Enzymes. *Antimicrobial Agents and Chemotherapy.* **2013**, *57* (12), 6074−80.
(30) Olakanmi, O.; Britigan, B. E.; Schlesinger, L. S. Gallium Disrupts Iron Metabolism of Mycobacteria Residing within Human Macrophages. *Infect. Immun.* **2000**, *68* (10), 5619.
(31) Hacht, B. Gallium(III) Ion Hydrolysis under Physiological Conditions. *Bulletin of the Korean Chemical Society.* **2008**, *29* (2), 372−6.
(32) Li, F.; Liu, F.; Huang, K.; Yang, S. Advancement of Gallium and Gallium-Based Compounds as Antimicrobial Agents. *Frontiers in Bioengineering and Biotechnology.* **2022**, *10*, 827960.
(33) Cvitkovic, F. R.; Armand, J. P.; Tubiana-Hulin, M.; Rossi, J. F.; Warrell, R. P. Randomized, double-blind, phase II trial of gallium

nitrate compared with pamidronate for acute control of cancer-related hyperealcemia. *Cancer Journal.* **2006**, *12* (1), 47−53.
(34) Warrell, R. P.; Coonley, C. J.; Straus, D. J.; Young, C. W. Treatment Of Patients With Advanced Malignant-Lymphoma Using Gallium Nitrate Administered As A 7-Day Continuous Infusion. *Cancer.* **1983**, *51* (11), 1982−7.
(35) Patra, J. K.; Das, G.; Fraceto, L. F.; Campos, E. V. R.; Rodriguez-Torres, M. D. P.; Acosta-Torres, L. S.; et al. Nano based drug delivery systems: recent developments and future prospects. *Journal of Nanobiotechnology.* **2018**, *16*, 71.
(36) Hunt, N. J.; Lockwood, G. P.; Kang, S. W. S.; Westwood, L. J.; Limantoro, C.; Chrzanowski, W.; et al. Quantum Dot Nanomedicine Formulations Dramatically Improve Pharmacological Properties and Alter Uptake Pathways of Metformin and Nicotinamide Mononucleotide in Aging Mice. *ACS Nano* **2021**, *15* (3), 4710−27.
(37) Nguyen, T-HT; Trinh, N.-T.; Tran, H. N.; Tran, H. T.; Le, P. Q.; Ngo, D.-N.; et al. Improving silymarin oral bioavailability using silica-installed redox nanoparticle to suppress inflammatory bowel disease. *Journal of controlled release.* **2021**, *331*, 515−24.
(38) He, M.; Protesescu, L.; Caputo, R.; Krumeich, F.; Kovalenko, M. V. A General Synthesis Strategy for Monodisperse Metallic and Metalloid Nanoparticles (In, Ga, Bi, Sb, Zn, Cu, Sn, and Their Alloys) via in Situ Formed Metal Long-Chain Amides. *Chem. Mater.* **2015**, *27* (2), 635−47.
(39) Dragoman, R. M.; Grogg, M.; Bodnarchuk, M. I.; Tiefenboeck, P.; Hilvert, D.; Dirin, D. N.; et al. Surface-Engineered Cationic Nanocrystals Stable in Biological Buffers and High Ionic Strength Solutions. *Chem. Mater.* **2017**, *29* (21), 9416−28.
(40) Pearson, R. G. HARD AND SOFT ACIDS AND BASES. *J. Am. Chem. Soc.* **1963**, *85* (22), 3533.
(41) PubChem Compound Summary for CID 65340, Dopamine hydrochloride [Internet]. 2021 [cited April 30, 2021]. Available from https://pubchem.ncbi.nlm.nih.gov/compound/Dopamine-hydrochloride.
(42) Zhu, H.; Prince, E.; Narayanan, P.; Liu, K.; Nie, Z.; Kumacheva, E. Colloidal stability of nanoparticles stabilized with mixed ligands in solvents with varying polarityElectronic supplementary information (ESI) available: Experimental methods and AuNP characterizations. *Chem. Commun.* **2020**, *56* (58), 8131−4.
(43) Swinehart, D. F. The Beer-Lambert Law. *Journal of chemical education.* **1962**, *39* (7), 333.
(44) Rzhepishevska, O.; Ekstrand-Hammarstrom, B.; Popp, M.; Bjorn, E.; Bucht, A.; Sjostedt, A.; et al. The Antibacterial Activity of Ga3+ Is Influenced by Ligand Complexation as Well as the Bacterial Carbon Source. *Antimicrobial Agents and Chemotherapy.* **2011**, *55* (12), 5568−80.
(45) de Leseleuc, L.; Harris, G.; KuoLee, R.; Chen, W. X. In Vitro and In Vivo Biological Activities of Iron Chelators and Gallium Nitrate against Acinetobacter baumannii. *Antimicrobial Agents and Chemotherapy.* **2012**, *56* (10), 5397−400.
(46) Miller, M. B.; Bassler, B. L. Quorum sensing in bacteria. *Annu. Rev. Microbiol.* **2001**, *55*, 165−99.
(47) Rutherford, S. T.; Bassler, B. L. Bacterial quorum sensing: its role in virulence and possibilities for its control. *Cold Spring Harb Perspect Med.* **2012**, *2* (11), a012427.
(48) O'Loughlin, C. T.; Miller, L. C.; Siryaporn, A.; Drescher, K.; Semmelhack, M. F.; Bassler, B. L. A quorum-sensing inhibitor blocks Pseudomonas aeruginosa virulence and biofilm formation. *Proceedings of the National Academy of Sciences.* **2013**, *110* (44), 17981−6.
(49) Lu, H. D.; Pearson, E.; Ristroph, K. D.; Duncan, G. A.; Ensign, L. M.; Suk, J. S.; et al. Pseudomonas aeruginosa pyocyanin production reduced by quorum-sensing inhibiting nanocarriers. *Int. J. Pharm.* **2018**, *544* (1), 75−82.
(50) Malešević, M.; Di Lorenzo, F.; Filipić, B.; Stanisavljević, N.; Novović, K.; Senerovic, L.; et al. Pseudomonas aeruginosa quorum sensing inhibition by clinical isolate Delftia tsuruhatensis 11304: involvement of N-octadecanoylhomoserine lactones. *Scientific Reports.* **2019**, *9* (1), 16465.
(51) Jayaseelan, S.; Ramaswamy, D.; Dharmaraj, S. Pyocyanin: production, applications, challenges and new insights. *World J. Microbiol. Biotechnol.* **2014**, *30* (4), 1159−68.
(52) Das, T.; Kutty, S. K.; Kumar, N.; Manefield, M. Pyocyanin Facilitates Extracellular DNA Binding to Pseudomonas aeruginosa Influencing Cell Surface Properties and Aggregation. *PLoS One* **2013**, *8* (3), e58299.
(53) Klare, W.; Das, T.; Ibugo, A.; Buckle, E.; Manefield, M.; Manos, J. Glutathione-Disrupted Biofilms of Clinical Pseudomonas aeruginosa Strains Exhibit an Enhanced Antibiotic Effect and a Novel Biofilm Transcriptome. *Antimicrob. Agents Chemother.* **2016**, *60* (8), 4539−51.
(54) Saunders, S. H.; Tse, E. C. M.; Yates, M. D.; Otero, F. J.; Trammell, S. A.; Stemp, E. D. A.; et al. Extracellular DNA Promotes Efficient Extracellular Electron Transfer by Pyocyanin in Pseudomonas aeruginosa Biofilms. *Cell.* **2020**, *182* (4), 919−32.
(55) Bastos, C. A. P.; Faria, N.; Wills, J.; Malmberg, P.; Scheers, N.; Rees, P.; et al. Copper nanoparticles have negligible direct antibacterial impact. *NanoImpact.* **2020**, *17*, 100192.
(56) Olson, M. E.; Ceri, H.; Morck, D. W.; Buret, A. G.; Read, R. R. Biofilm bacteria: formation and comparative susceptibility to antibiotics. *Can. J. Vet Res.* **2002**, *66* (2), 86−92.
(57) Sheng, X.; Ting, Y. P.; Pehkonen, S. O. The influence of ionic strength, nutrients and pH on bacterial adhesion to metals. *J. Colloid Interface Sci.* **2008**, *321* (2), 256−64.
(58) Toyofuku, M.; Inaba, T.; Kiyokawa, T.; Obana, N.; Yawata, Y.; Nomura, N. Environmental factors that shape biofilm formation. *Biosci., Biotechnol., Biochem.* **2016**, *80* (1), 7−12.
(59) Silhavy, T. J.; Kahne, D.; Walker, S. The bacterial cell envelope. *Cold Spring Harbor perspectives in biology.* **2010**, *2* (5), a000414.
(60) Yang, D. C.; Blair, K. M.; Salama, N. R. Staying in Shape: the Impact of Cell Shape on Bacterial Survival in Diverse Environments. *Microbiology and Molecular Biology Reviews.* **2016**, *80* (1), 187−203.
(61) Mah, T-FC; O'Toole, G. A. Mechanisms of biofilm resistance to antimicrobial agents. *Trends in Microbiology.* **2001**, *9* (1), 34−9.
(62) Lee, J.-H.; Regmi, S. C.; Kim, J.-A.; Cho, M. H.; Yun, H.; Lee, C.-S.; et al. Apple Flavonoid Phloretin Inhibits Escherichia coli O157:H7 Biofilm Formation and Ameliorates Colon Inflammation in Rats. *Infect. Immun.* **2011**, *79* (12), 4819−27.
(63) Payne, D. E.; Martin, N. R.; Parzych, K. R.; Rickard, A. H.; Underwood, A.; Boles, B. R. Tannic Acid Inhibits Staphylococcus aureus Surface Colonization in an IsaA-Dependent Manner. *Infect. Immun.* **2013**, *81* (2), 496−504.
(64) Roy, R.; Tiwari, M.; Donelli, G.; Tiwari, V. Strategies for combating bacterial biofilms: A focus on anti-biofilm agents and their mechanisms of action. *Virulence.* **2018**, *9* (1), 522−54.
(65) Harrison, J. J.; Ceri, H.; Stremick, C.; Turner, R. J. Differences in biofilm and planktonic cell mediated reduction of metalloid oxyanions. *FEMS microbiology letters.* **2004**, *235* (2), 357−62.
(66) Jiang, Q.; Chen, J.; Yang, C.; Yin, Y.; Yao, K. Quorum Sensing: A Prospective Therapeutic Target for Bacterial Diseases. *Biomed Res. Int.* **2019**, *2019*, 2015978.
(67) Kurtuldu, F.; Mutlu, N.; Boccaccini, A. R.; Galusek, D. Gallium containing bioactive materials: A review of anticancer, antibacterial, and osteogenic properties. *Bioactive Materials.* **2022**, *17*, 125−46.
(68) Rochford, E. T. J.; Richards, R. G.; Moriarty, T. F. Influence of material on the development of device-associated infections. *Clinical Microbiology and Infection.* **2012**, *18* (12), 1162−7.
(69) Shruti, S.; Andreatta, F.; Furlani, E.; Marin, E.; Maschio, S.; Fedrizzi, L. Cerium, gallium and zinc containing mesoporous bioactive glass coating deposited on titanium alloy. *Appl. Surf. Sci.* **2016**, *378*, 216−23.
(70) Stuart, B. W.; Stan, G. E.; Popa, A. C.; Carrington, M. J.; Zgura, I.; Necsulescu, M.; et al. New solutions for combatting implant bacterial infection based on silver nano-dispersed and gallium incorporated phosphate bioactive glass sputtered films: A preliminary study. *Bioactive Materials.* **2022**, *8*, 325−40.

NOTE ADDED AFTER ASAP PUBLICATION

This article was published ASAP on March 28, 2023. The Table of Contents and Abstract graphics have been updated and the corrected version was reposted on March 31, 2023.

https://doi.org/10.1021/acsmaterialsau.2c00078
ACS Mater. Au 2023, 3, 310−320